

Comparison of Keldysh models with numerical experiments on above-threshold ionization

J. Javanainen

Department of Physics, University of Connecticut, Storrs, Connecticut 06268

J. H. Eberly

Department of Physics and Astronomy, University of Rochester, Rochester, New York 14627

(Received 24 August 1988)

We compute above-threshold ionization electron spectra by solving numerically the time-dependent Schrödinger equation of a one-dimensional model atom in an external field, and compare the results with three Keldysh-type models worked out for the same atom. The Keldysh models offer an unreliable representation of the ionization process.

The phenomenon that the energy spectrum of electrons liberated in high-intensity multiphoton ionization exhibits a succession of peaks separated by photon energy [above-threshold ionization (ATI)] is now represented by a large body of rather well-unified experimental work.^{1,2} On the theoretical side the situation is less settled. Variations of the idea originally due to Keldysh,³ now sometimes referred to as the Keldysh-Faisal-Reiss³⁻⁵ (KFR) approach, have been generally accepted as providing the best frame of thinking about ATI. So far, however, the success met by KFR theories has not been conclusive,⁶ and experiments specifically dedicated to quantitative comparisons of photoelectron spectra with KFR predictions are just beginning to be made.⁷

Direct numerical solutions of the Schrödinger equations of (often) one-dimensional model atoms constitute an alternative theoretical strategy rapidly gaining ground in multiphoton physics.⁸⁻¹¹ These simulations have the potential to supplement or replace traditional methods such as finite-order perturbation theory and strong-coupling analysis of resonances, whose validity is dubious at high intensities in multistate atoms. From another angle, simulations can also be viewed simply as numerical experiments and compared with KFR theories.^{8,10,11} Here we report on an *absolute comparison* between numerical simulations and three KFR models worked out for the same atom. The qualitative and quantitative agreements turn out unsatisfactory.

Our one-dimensional model atom is defined by the Hamiltonian

$$H_0 = -\frac{1}{2} \frac{\partial^2}{\partial x^2} - \frac{1}{(1+x^2)^{1/2}}. \quad (1)$$

Thanks to the Coulomb tail of the binding potential, this model exhibits many characteristics of real atoms such as Rydberg series of excited states and bound-free coupling matrix elements that extrapolate continuously across the continuum limit. Moreover, the potential is regular at the origin, which further enhances the similarity with ordinary atoms: We may define our atom on the entire real axis, parity is a good quantum number, and bound states do not have permanent dipole moments.

We add to the Hamiltonian H_0 a dipole interaction with an external field, $H_{\text{int}} = -xE \sin(\omega t)$, and integrate

the time-dependent Schrödinger equation starting from the bare ground state $\psi_g(x)$ of H_0 up to the desired interaction time T by applying the standard Crank-Nicholson algorithm. Finally, we form the photoelectron energy spectrum $P(W) = |\langle W | \psi(T) \rangle|^2$ by projecting the time-dependent wave function $\psi(x, T)$ onto the positive-energy bare eigenstates $\psi_W(x)$ of H_0 .

We shall discuss photoelectron spectra in nominal ten-photon ionization for the field frequency $\omega = 0.07$. In practice, our computations are carried out on a 32767-point spatial grid with step size 0.0707. Here, we present data for the interaction time $T = 740.52$, i.e., 8.25 cycles of the laser field.

In Fig. 1(a) we plot the computed photoelectron energy spectrum for the field strength $E = 0.07071$. It shows a number of ATI peaks. To characterize the results in a compact way, we derive from the spectrum $P(W)$ and from the position of the lowest peak W_0 the total ionization probability P , the effective ionization rate R and a quantity representing the number of ATI peaks N , as follows:

$$P = \int_0^\infty dW P(W), \quad (2a)$$

$$R = -\ln(1-P)/T, \quad (2b)$$

$$N = \frac{1}{\omega} \left[\frac{1}{P} \int_0^\infty dW P(W) W - W_0 \right]. \quad (2c)$$

They are given in Table I for $E = 0.07071$, and also for $E = 0.05$, $E = 0.1$. These field strengths approximately cover the range where our simulations produce good-quality ATI spectra for the given frequency ω .¹¹ Perhaps it is not a coincidence that they also approximately cover the range of E from where the ponderomotive potential $V_P = E^2/4\omega^2$ becomes comparable to the photon energy, up to the classical limit of static-field ionization.

Details^{11,12} of the computations, including the choices of the $x \cdot E$ length gauge and of the interaction times,¹¹ as well as our earlier results,¹¹ are described elsewhere. We are now able to report reasonably accurate spectra at an interaction time longer than those in Ref. 11, because we have (at the expense of a substantial increase in CPU time) extensively investigated the numerical truncation errors by varying the iteration parameters of the time in-

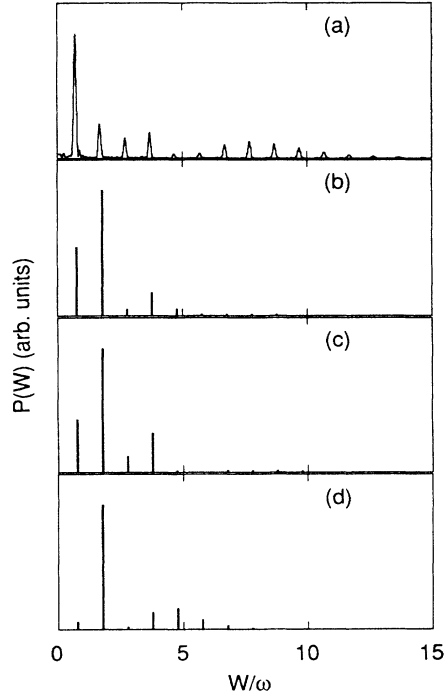


FIG. 1. Photoelectron energy spectra for nominal ten-photon ionization with field frequency $\omega=0.07$ and strength $E=0.07071$. (a) shows the simulation result obtained at the interaction time of 8.25 field cycles, while (b)–(d) display the relative heights of the ATI peaks from the theories KFR1 [adapted from Reiss (Ref. 5)], KFR2 [adapted from Keldysh (Ref. 3)], and KFR3 [adapted from Basile *et al.* (Ref. 14)], respectively.

tegration. Specifically, the time step was decreased until convergence was verified. For $E=0.07071$ we also varied the number of, and distance between, the spatial grid points, which showed that the remaining errors in R and N due to discretization of space are of the order of 10%. In addition to numerical errors, systematic effects may bias the results. It is difficult to estimate how much R and N depend on the interaction time, because at the current computer capacity even the numerical accuracy cannot be assessed for interaction times longer than about 8 cycles. However, on the basis of our experience with lower-order ionization¹¹ and comparisons with the results obtained for

4.25 cycles,¹² we believe that the qualitative shape of the spectrum in Fig. 1(a) ensues for much longer pulses as well, and that for longer pulses the variation of the quantities R and N in Table I would be a few tens of percent.

We now turn to the KFR approach to ATI.^{3–5,13–15} The basic idea is to couple the ground-state wave function $\psi_g(x,t) = \psi_g(x) \exp(-iW_g t)$ to “photon-dressed” continuum states $\psi_W(x,t)$ which already incorporate part of the laser-electron interaction. The transition amplitude to the continuum state W at time t is written

$$a(W,t) = -i \int_0^t dt \int dx \psi_W^*(x,t) H_{\text{int}}(x,t) \psi_g(x,t). \quad (3)$$

Different approximations of laser-dressed continuum wave functions $\psi_W(x,t)$ produce different transition rates. Also, the original KFR models^{3–5,13,14} are built on a direct dipole coupling of the ground state to the continuum, while some current refinements¹⁵ use as H_{int} an effective multiphoton interaction that attempts to take into account other bound states in addition to the ground state.

We have adapted three KFR models based on direct ionization of the ground state to our one-dimensional atom:

(1) *KFR1*. $H_{\text{int}} = p \cdot A + \frac{1}{2} A^2$ dipole interaction, one-dimensional free-electron Volkov states computed in the velocity gauge are used as $\psi_W(x,t)$ [but the ground-state wave function is still just $e^{-iW_g t} \psi_g(x)$]. This is the Reiss version⁵ of KFR. In the long-time limit the ATI peaks become δ functions, and the partial transition rate to the peak $S=0,1,2,\dots$ is

$$R_S = \pi \left| (W + V_I) \frac{1}{\sqrt{2\pi p}} \int dx e^{-ipx} \psi_g(x) \times \sum_l J_{K+2l} \left(\frac{pE}{\omega^2} \right) J_l \left(\frac{E^2}{8\omega^3} \right) \right|^2. \quad (4)$$

Here K is the true multiphoton order of the peak S , given in terms of the ionization potential $V_I = -W_g = 0.670$ and the ponderomotive upshift of the ionization threshold $V_P = E^2/4\omega^2$ as the smallest integer larger than

TABLE I. Comparison of numerical simulations (sim) and three KFR models of ATI in ten-photon ionization of a model atom. The simulation data are for 8.25 cycles of the driving field. The numerical error in the simulations, estimated to be 10% for $E=0.07071$, mainly comes from the spatial step size 0.0707 used in the computations; the KFR results are believed to be accurate to within ± 1 in the last digit displayed. The notation $d[e]$ stands for $d \times 10^{-e}$.

E	P		R			N			
	sim	sim	KFR1	KFR2	KFR3	sim	KFR1	KFR2	KFR3
0.05	2.6[3]	3.5[6]	6.0[9]	5.1[8]	6.3[9]	3.0	0.2	0.2	0.4
0.07071	1.4[1]	2.0[4]	2.0[7]	1.5[6]	3.7[7]	2.6	1.0	1.4	1.8
0.1	8.0[1]	2.2[3]	1.9[5]	1.6[4]	3.7[5]	4.1	0.9	1.2	2.3

$S + (V_I + V_P)/\omega$. $W = K\omega - (V_I + V_P)$ and $p = (2W)^{1/2}$ are the corresponding energy and momentum of the photoelectron spectrum peak S , and J stands for Bessel functions of the first kind.

(2) *KFR2*. $x \cdot E$ length gauge of the dipole interaction (as in the simulations), free-electron Volkov states computed in the $x \cdot E$ interaction are used as $\psi_W(x, t)$. This is the original choice of Keldysh.³

(3) *KFR3*. $x \cdot E$ gauge, $\exp(ip \cdot x)$ part of the Volkov

state is replaced by the exact continuum eigenstate $\psi_W(x)$ with $W = p^2/2$.¹⁴ This improvement of the Keldysh model inserts as much of the atomic structure as is easily feasible. In one-photon ionization at low intensities KFR3 gives back the golden-rule ionization rate, a fact that was profitably utilized to debug normalization factors in our computer programs.

With the same notation as in Eq. (4), the partial ionization rates for KFR2 and KFR3 read

$$R_S = \pi\omega^2 \left| \sum_{\substack{k,l,m \\ k+l+2m=K}} ki^{-k} \left[\int dx u_W^*(x) J_k \left(-\frac{x E}{\omega} \right) \psi_g(x) \right] J_l \left(\frac{p E}{\omega^2} \right) J_m \left(\frac{-E^2}{8\omega^3} \right) \right|^2, \quad (5)$$

where $u_W(x)$ stands either for the energy-normalized plane wave (KFR2) or for $\psi_W(x)$ (KFR3). We have implemented Eq. (5) as it stands, except for one technical point. Namely, owing to the reflecting boundary conditions at the ends of the spatial region allotted for the wave functions, the spectrum of H_0 is discrete and the positive-energy wave functions $\psi_W(x)$ come out alternately even and odd. Analogous to the definition of the electron spectrum in the simulations,¹¹ we have averaged the transition rates computed from (5) for the even and the odd state closest to W .

The electron spectra of models KFR1-KFR3 are plotted in the respective Figs. 1(b)-1(d) for $E = 0.07071$, and the ensuing total ionization rates R and numbers of ATI peaks N are listed in Table I for $E = 0.05, 0.07071$, and 0.1 .

Among themselves, the three KFR models give similar spectra, even at low energies where the continuum wave function in KFR3 is quite different from KFR1 and KFR2, and the intensity scalings (although not absolute values) of the ionization rates are almost identical. Finally, the peak positions in the KFR models closely agree with the simulation results, in agreement with the picture that at low laser frequencies the dynamical threshold shift nearly equals the ponderomotive potential.^{2,11}

On the other hand, the electron spectra and the number of ATI peaks in the simulations and in the KFR models differ quite erratically. Basically, the spectrum extends to higher energies in the simulations than in the KFR models. The ionization rates and the intensity scalings of the ionization rates are also markedly different between the simulations and the KFR models.

For ten-photon ionization of our model atom in an intensity range covering about three orders of magnitude in the ionization rate, the KFR models give the peak positions correctly but otherwise their predictions bear little qualitative or quantitative resemblance to the numerical simulations.

While we have worked in one dimension and the outcome of the comparison need not directly apply to real atoms, at the very least we may recommend extreme caution: The value of a KFR model of ATI as an argument is questionable unless the limits of validity of the model are explicitly known. Comparison of our simulation results with those KFR theories where the electron bridges the bound states with the aid of an effective multiphoton matrix element¹⁵ might be more rewarding than studies of direct-ionization models. However, we do not know at present how to derive a quantitative multiphoton matrix element for, say, $E = 0.1$, when the field-induced upshift of the continuum threshold is so large that the minimum multiphoton order required to ionize the atom has actually increased from 10 to 17.

This work was supported by grants from the National Allocation Committee of the John von Neumann Center for time on a Cyber 205 computer. We are also grateful to Phillip Gould for the loan of one of the Macintosh II microcomputers employed in the KFR calculations, to Winthrop Smith for helpful comments on the manuscript, and to Qichang Su for technical assistance in the computations. One of us (J.J.) would especially like to acknowledge helpful dialogue with Howard Reiss.

¹P. Agostini, F. Fabre, G. Mainfray, G. Petite, and N. K. Rahman, *Phys. Rev. Lett.* **42**, 1127 (1979); P. Kruit, J. Kimman, H. G. Muller, and M. J. van der Wiel, *Phys. Rev. A* **28**, 248 (1983); L. A. Lompré, A. L'Huillier, G. Mainfray, and C. Manus, *J. Opt. Soc. Am. B* **2**, 1906 (1985); U. Johann, T. S. Luk, H. Egger, and C. K. Rhodes, *Phys. Rev. A* **34**, 1084 (1986); H. J. Humpert, H. Schwier, R. Hippler, and H. O. Lutz, *ibid.* **32**, 3787 (1985); R. R. Freeman, T. J. McIlrath, P. H. Bucksbaum, and M. Bashkansky, *Phys. Rev. Lett.* **57**, 3156 (1986).

²P. Agostini, J. Kupersztych, L. A. Lompré, G. Petite, and F. Yergeau, *Phys. Rev. A* **36**, 4111 (1987); R. R. Freeman, P. H. Bucksbaum, H. Milchberg, S. Darack, D. Schumacher, and M. E. Geusic, *Phys. Rev. Lett.* **59**, 1092 (1987); H. G. Muller, H. B. van den Linden van den Heuvell, P. Agostini, G. Petite, A. Antonetti, M. Franco, and A. Migus, *ibid.* **60**, 565 (1988).

³L. V. Keldysh, *Zh. Eksp. Teor. Fiz.* **47**, 1945 (1964) [*Sov. Phys. JETP* **20**, 1307 (1965)].

⁴F. Faisal, *J. Phys. B* **6**, L312 (1973).

- ⁵H. R. Reiss, Phys. Rev. A **22**, 1786 (1980).
- ⁶M. D. Perry, O. L. Landen, A. Szöke, and E. M. Campbell, Phys. Rev. A **37**, 747 (1988); H. R. Reiss, J. Opt. Soc. Am. B **4**, 726 (1987); M. Bashkansky, P. H. Bucksbaum, and D. W. Schumacher, Phys. Rev. Lett. **60**, 2458 (1988).
- ⁷G. Petite (private communication).
- ⁸S. Geltman, J. Phys. B **10**, 831 (1977); H. S. Antunes Neto, L. Davidovich, and D. Marchesin, in *Coherence and Quantum Optics V*, edited by L. Mandel and E. Wolf (Plenum, New York, 1984).
- ⁹K. C. Kulander, Phys. Rev. A **35**, 445 (1987); **36**, 2726 (1987); **38**, 778 (1988); C. Cerjan and R. Kosloff, J. Phys. B **20**, 4441 (1987); M. S. Pindzola and C. Bottcher, J. Opt. Soc. Am. B **4**, 752 (1987); R. Shakeshaft and M. Dörr, Z. Phys. D **8**, 255 (1988); S. M. Susskind and R. V. Jensen, Phys. Rev. A **38**, 711 (1988); B. Sundaram and L. Armstrong, Jr., *ibid.* **38**, 152 (1988).
- ¹⁰L. A. Collins and A. L. Merts, Phys. Rev. A **37**, 2415 (1988).
- ¹¹J. Javanainen and J. H. Eberly, J. Phys. B **21**, L93 (1988); J. H. Eberly and J. Javanainen, Phys. Rev. Lett. **60**, 1346 (1988); J. Javanainen, J. H. Eberly, and Q. Su, Phys. Rev. A **38**, 3430 (1988).
- ¹²J. Javanainen, J. H. Eberly, and Q. Su (unpublished).
- ¹³M. Lewenstein, J. Mostowski, and M. Trippenbach, J. Phys. B **18**, L461 (1985).
- ¹⁴S. Basile, F. Trombetta, G. Ferrante, R. Burlon, and C. Leone, Phys. Rev. A **37**, 1050 (1988).
- ¹⁵A. Dulcic, Phys. Rev. A **35**, 1673 (1987); W. Becker, R. R. Schlicher, and M. O. Scully, J. Phys. B **19**, L785 (1986); R. Shakeshaft and R. M. Potvliege, Phys. Rev. A **36**, 5478 (1987).